A review of the use of magnetic resonance imaging in Parkinson's disease

Nadya Pyatigorskaya, Cécile Gallea, Daniel Garcia-Lorenzo, Marie Vidailhet and Stéphane Lehericy

Ther Adv Neurol Disord
2014, Vol. 7(4) 206–220
DOI: 10.1177/1756285613511507

***Abstract*:** To date, the most frequently used Parkinson's disease (PD) biomarkers are the brain imaging measures of dopaminergic dysfunction using positron emission tomography and single photon emission computed tomography. However, major advances have occurred in the development of magnetic resonance imaging (MRI) biomarkers for PD in the past decade. Although conventional structural imaging remains normal in PD, advanced techniques have shown changes in the substantia nigra and the cortex. The most well-developed MRI markers in PD include diffusion imaging and iron load using T2/T2* relaxometry techniques. Other quantitative biomarkers such as susceptibility-weighted imaging for iron load, magnetization transfer and ultra-high-field MRI have shown great potential. More sophisticated techniques such as tractography and resting state functional connectivity give access to anatomical and functional connectivity changes in the brain, respectively. Brain perfusion can be assessed using non-contrast-agent techniques such as arterial spin labelling and spectroscopy gives access to metabolites concentrations. However, to date these techniques are not yet fully validated and standardized quantitative metrics for PD are still lacking. This review presents an overview of new structural, perfusion, metabolic and anatomo-functional connectivity biomarkers, their use in PD and their potential applications to improve the clinical diagnosis of Parkinsonian syndromes and the quality of clinical trials.

Keywords: diffusion tensor imaging, magnetization transfer, relaxometry, resting state fMRI

Corresponding author:
Stéphane Lehericy, MD, PhD, CENIR-ICM
Service de neuroradiologie, Groupe Hospitalier Pitié-Salpêtrière, 47 boulevard de l'hopital, 75651 Paris cedex 13, France
stephane.lehericy@psl.aphp.fr

Nadya Pyatigorskaya
MD Institut du Cerveau et de la Moelle épinière, Centre de Neuroimagerie de Recherche, Paris, France
Service de neuroradiologie, Groupe Hospitalier Pitié-Salpêtrière, Paris, France

Cécile Gallea, PhD
Daniel Garcia-Lorenzo, PhD
Institut du Cerveau et de la Moelle épinière, Centre de Neuroimagerie de Recherche, Paris, France
Université Pierre et Marie Curie (UPMC Univ Paris 6), Centre de Recherche de l'Institut du Cerveau et de la Moelle epiniere, Paris, France

Marie Vidailhet, MD
Université Pierre et Marie Curie (UPMC Univ Paris 6), Centre de Recherche de l'Institut du Cerveau et de la Moelle epiniere, Paris, France
Federation de Neurologie, Groupe Hospitalier Pitié-Salpêtrière, Paris, France

Introduction

The diagnosis of Parkinson's disease (PD) is mainly based on clinical features and does not rely on imaging biomarkers. Commonly used imaging techniques in PD include positron emission tomography (PET) and single photon emission computed tomography (SPECT), but conventional magnetic resonance imaging (MRI) is of little use in clinical practice. However, advances in structural and functional imaging have improved the capacity of MRI to detect changes in PD as well as to differentiate between PD and other Parkinsonian syndromes. MRI has provided several candidate biomarkers that have a potential to inform on the disease process. Biomarkers are quantitative characteristics which are used as indicators of biological or pathological states. In neuroimaging, biomarkers are measures derived from images that reflect the presence of diseases or their severity and that can be used for early diagnosis, prognosis or to monitor responses to therapeutic interventions. Biomarkers are expected to detect early neuropathological features and mechanisms underlying neurodegeneration in PD and to correlate with disease progression in order to allow the monitoring of disease status. Ideally, they should be able to detect preclinical changes. Reliable biomarkers need to be confirmed by independent studies.

Promising candidate biomarkers were able to detect changes at various levels of the central nervous system, including the substantia nigra (SN), the brainstem, the basal ganglia and the cortex. New MR contrasts and image analysis techniques have improved the visualization of the SN and other brainstem nuclei. Cortical lesions can be followed using various techniques that can detect changes in the thickness, volume and density of grey matter in the cortex. Quantitative imaging

Table 1. MRI techniques.

Method	Techniques	Information	Changes in PD
Structural	T1-w, T2-w, IR, MT	Morphometry	SN: variable volume changes Cortex: mild reduction in volume and thickness
Neuromelanin	Spin echo T1-w	Presence of melanin-containing cells	Reduced signal intensity
Magnetization transfer	Images with (M_T) and without (M_0) MT pulse	Degree of myelination, axonal density	Reduced MT ratio (MTR = $M_0 - M_T/M_0$)
Relaxometry	T2/T2* measurements	Brain iron	Reduced T2/T2* Increased R2/R2*
Susceptibility-weighted	Phase images	Brain iron	Increased susceptibility due to iron load
Diffusion	DTI	Diffusion of water in biological tissues	Reduced FA
Tractography	DTI	Fibre tract-specific reconstruction	Reduced probability of connections
Functional	Resting state BOLD fMRI	Functional connectivity within brain networks	Reduced FC in sensorimotor Increased FC in associative
MR spectroscopy	^{1}H MRS	NAA, Cho, mIns, GABA, Glx, GSH, lactate	Trend for metabolite reduction
	^{31}P MRS	Energy metabolism: ADP, PCr/ATP	Decreased ATP in midbrain
Perfusion	ASL	rCBF	Reduced in cortex, Variable in basal ganglia

^{1}H MRS, proton magnetic resonance spectroscopy; ^{31}P MRS, phosphorus magnetic resonance spectroscopy; ADP, adenosine diphosphate; ASL, arterial spin labelling; ATP, adenosine triphosphate; BOLD, blood oxygen level-dependent contrast; Cho, choline-containing compounds; DTI, diffusion tensor imaging; FA, fractional anisotropy; FC, functional connectivity; fMRI, functional magnetic resonance imaging; Glx, glutamate/glutamine; GSH, glutathione; IR, inversion recovery; mIns, *myo*-inositol; MT, magnetization transfer; MTR, magnetization transfer ratio; NAA, *N*-acetylaspartate; rCBF, regional cerebral blood flow; PCr, phosphocreatine; SN, substantia nigra; T2, T2 relaxation time; T2*, gradient echo T2 relaxation time; T1-w, T1-weighted; T2-w, T2-weighted; R2, T2 relaxation rate; R2*, T2* relaxation rate.

includes techniques such as relaxometry, susceptibility-weighted, diffusion and magnetization transfer (MT) imaging. Perfusion can be assessed using non-contrast-agent technique MRI and brain metabolism using magnetic resonance spectroscopy. Tractography was used to investigate anatomical connectivity and resting state functional MRI (rsfMRI) provides new information on functional connectivity changes in the brain of PD patients. Task-related activation functional MRI (fMRI) will not be reviewed here. In the SN, although most MRI biomarker candidates were not validated in experimental models and require confirmation in independent studies, it is clear that they have the potential to quantify the pathology and follow the disease progression of PD.

This article reviews new MRI techniques and their use in PD and explains how these techniques may be used to detect changes in the brain of PD patients and their relationships with Parkinsonian symptoms. A summary of these techniques is presented in Table 1 and Figure 1. Each imaging technique and their respective contribution to the study of PD will be presented in the following sections. They include structural imaging, techniques that can assess iron load, other quantitative techniques (e.g. MT, diffusion imaging), perfusion imaging, magnetic resonance spectroscopy and techniques that can assess anatomical and functional connectivity. For the review, the authors searched PubMed from 1990 until early 2013 by using the terms corresponding to each technique and the terms corresponding to the pathological conditions, i.e. Parkinson's disease and related atypical Parkinsonian conditions.

Structural imaging

Techniques for visualization and segmentation of brain regions

MRI sequences for visualization of the basal ganglia and the cortex. Conventional three-dimensional T1-weighted (T1-w) sequences present high grey/white matter contrast for cortical and some basal ganglia structures, but poor contrast in many structures of interest in PD (SN, subthalamic

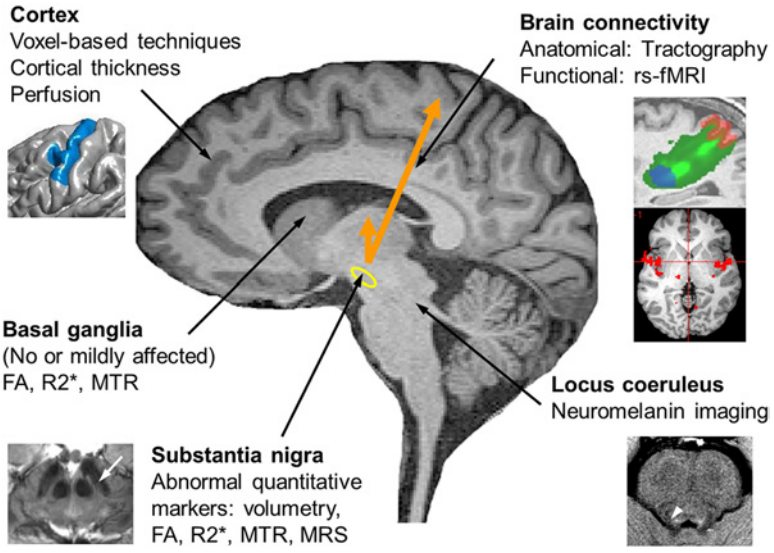

Figure 1. Overview of MRI methods used to study PD. Cortex: changes were detected using voxel-based techniques, cortical thickness measurements and perfusion imaging. Brain connectivity was investigated using resting-state functional MRI (rs-fMRI) for functional connectivity and tractography for structural connectivity. Substantia nigra (yellow contour): changes were detected using diffusion imaging (reduced fractional anisotropy - FA), relaxometry (increased R2* indicating increased iron load and more recently susceptibility-weighted imaging), magnetization transfer ratio (MTR reduced) and spectroscopy. Basal ganglia: studies showed no or mild changes in FA, R2* or MTR. Locus coeruleus area (white arroxw head): reduced signal intensity was detected using neuromelanin imaging.

nucleus [STN], globus pallidus [GP], red nucleus [RN]). These latter structures contain high iron levels leading to shortened T1 and reduced contrast [Hardy *et al.* 2005]. Iron load is an advantage in T2-w and T2*-w sequences that use the T2 shortening effects of iron providing enhanced contrast. Susceptibility-weighted imaging (SWI) is promising in PD due to its improved sensitivity to brain mineralization [Haacke *et al.* 2005]. SWI uses the magnetic susceptibility differences in brain tissues [Haacke *et al.* 2005; Lotfipour *et al.* 2012; Schafer *et al.* 2012; Wang *et al.* 2012]. SWI images are sensitive to iron concentration and improve visualization of the SN [Haacke *et al.* 2005; Lotfipour *et al.* 2012; Schafer *et al.* 2012; Wang *et al.* 2012]. Proton-density and short tau inversion recovery (STIR) images were suggested as good alternatives. Other contrasts, such as the MT [Helms *et al.* 2009; Menke *et al.* 2010] and inversion recovery sequences [Hutchinson *et al.* 2003] also improved visualization of the SN. MT pulses increase contrast between the SN and the surrounding white matter, resulting in more accurate delineation and improved visualization of these structures [Helms *et al.* 2009; Menke *et al.* 2010]. Lastly, the increase in magnetic field provided by 7T human MRI, provided not only increased spatial resolution but also improved contrast, which allowed better visualization of basal ganglia contours and shapes. The volume and contours of the SN depend on the MRI contrast that was used [Oikawa *et al.* 2002]. For instance, contours that were shown using the T2-w sequences, which are sensitive to iron load, probably differed from those detected using inversion recovery and neuromelanin imaging.

The anatomy of the cortex is usually better depicted using conventional three-dimensional T1-weighted sequences which present high grey/white matter contrast.

Segmentation and volume calculation. Small structures such as the SN are usually outlined and segmented manually. Some cortical regions (e.g. the hippocampus, the striatum and the thalamus) can be segmented manually, but automated techniques are preferred as exploratory tools to detect grey and white matters changes in the cortex [Destrieux *et al.* 2010; Patenaude *et al.* 2011]. These techniques are designed for group studies, are automated, whole brain and rater independent. They include voxel-based, deformation-based and tensor-based morphometry, cortical thickness and sulci measurements. Voxel-based morphometry (VBM) is now a standard

technique, sensitive to differences in grey and white matter [Ashburner and Friston, 2000]. VBM provides metrics such as the concentration, density and volume of grey matter. A major limitation of VBM is the nonspecificity with respect to the underlying tissue changes. Deformation-based and tensor-based morphometry provide information about global or local differences in shape, respectively [Apostolova and Thompson, 2007; Good *et al.* 2001]. Other software allows measurements of topographic differences in thickness, surface area and curvature of the cortex [Dale *et al.* 1999; Fischl *et al.* 1999; Makris *et al.* 2005].

Volume and shape changes in Parkinson disease

Substantia nigra. The volume of the SN is usually measured using manual segmentation. Results in PD are discordant with normal [Oikawa *et al.* 2002; Peran *et al.* 2010], reduced [Hutchinson *et al.* 2003; Menke *et al.* 2009; Minati *et al.* 2007] and even increased volumes [Cho *et al.* 2011; Kwon *et al.* 2012] (Table 1). The origin of this variability is probably due to differences in methodology between studies. First, the variability of volume measurements is large, given the small size of the structure. Second, different contrasts were used resulting in changes in SN contours. Third, some methods relied on tractography and anatomical connectivity changes which are completely different in nature as compared with other structural methods. Lastly, increased SN volume was obtained using 7T imaging and may be explained by the increased volume of regions with iron load. Inversion recovery methods were able to detect a predominant involvement of the lateral segments of the SN [Hutchinson *et al.* 2003; Minati *et al.* 2007] in line with the preferential degeneration of dopaminergic neurons in the caudal and lateral SN in histological studies [Redgrave *et al.* 2010]. Overall, although volume changes were detected in the SN of PD patients, changes varied between studies and the reproducibility was low. Ultra-high-field MRI may provide improved results due to increased spatial resolution.

Other basal ganglia and brainstem nuclei. Global measurements of brainstem volumes [Longoni *et al.* 2011; Oba *et al.* 2005] and rate of atrophy [Paviour *et al.* 2006] were usually normal in PD patients. Similarly, most studies did not find any global volumetric changes in the basal ganglia [Bonneville *et al.* 2005; Oba *et al.* 2005; Paviour *et al.* 2006]. Neuromelanin-sensitive imaging showed reduced signal intensity in the locus coeruleus in PD patients compared with controls, probably reflecting loss of neuromelanin-containing neurons [Sasaki *et al.* 2006] (Table 1). A reduction in signal intensity in the locus coeruleus/subcoeruleus area correlated with the percentage of atonia during rapid eye movement (REM) sleep suggesting that damage to this region is implicated in the pathophysiology of REM sleep behaviour disorder [Garcia-Lorenzo *et al.* 2013].

Cortex. The understanding of brain mechanisms underlying cognitive impairment is of particular interest in PD. Mild cognitive impairment is common in nondemented PD patients and is a risk factor of progression to dementia, which develops in about 30% of PD patients [Litvan *et al.* 2011; Svenningsson *et al.* 2012]. Impaired cognition in PD has a heterogeneous profile including attention, executive, visuospatial and memory deficits [Svenningsson *et al.* 2012]. Different lesions may explain the different cognitive deficits [Brooks and Pavese, 2010]. Executive dysfunction may be related to dopaminergic fronto-subcortical deficits whereas dementia may be associated with widespread atrophy in posterior parietal and temporal cortical areas, associated with Lewy body deposition or Alzheimer plaques, and with nondopaminergic neurotransmitter dysfunctions such as cholinergic deficiency [Brooks and Pavese, 2010; Ibarretxe-Bilbao *et al.* 2009, 2011a; Svenningsson *et al.* 2012]. Structural MRI is a powerful technique to detect cortical changes in PD and evidence for cortical damage will be presented below.

Nondemented cognitively intact PD. Cortical morphology in cognitively intact PD patients may be normal [Cerasa *et al.* 2011; Feldmann *et al.* 2008; Messina *et al.* 2011; Paviour *et al.* 2006; Rizzo *et al.* 2008; Seppi and Poewe, 2010; Tessitore *et al.* 2012a] or altered in frontal regions [Biundo *et al.* 2011; Burton *et al.* 2004; Karagulle Kendi *et al.* 2008] or in more widespread cortical regions including parietal, temporal and occipital areas [Jubault *et al.* 2011; Lyoo *et al.* 2010; Meppelink *et al.* 2010; Tinaz *et al.* 2011]. Variations may be related to changes in methodology or disease stage but changes were most often mild. Cortical atrophy in fronto-temporal regions accelerates with disease progression [Ibarretxe-Bilbao *et al.* 2012].

Mild cognitive impairment and dementia. In contrast, impaired cognition and dementia in PD were associated with more severe patterns of cortical atrophy [Beyer *et al.* 2007; Burton *et al.*

2004] as reviewed by Ibarretxe-Bilbao and colleagues [Ibarretxe-Bilbao *et al.* 2009, 2011a]. Regions predictive of cognitive decline included the hippocampus and parieto-temporal regions [Weintraub *et al.* 2012]. The Alzheimer's disease pattern of brain atrophy may thus be a preclinical biomarker of impaired cognition in PD patients.

Cortical correlates of other nonmotor dysfunctions. Apart from impaired cognition and dementia, other nonmotor symptoms in PD include mood disorders, psychotic symptoms, hyposmia and sleep disorders [Brooks and Pavese, 2010]. Depression in PD patients was associated with structural changes in the limbic system including medial, orbitofrontal and temporal regions [Feldmann *et al.* 2008; Kostic *et al.* 2010] and the mediodorsal thalamus [Cardoso *et al.* 2009]. Visual hallucinations were associated with atrophy in limbic, paralimbic and neocortical areas in some studies [Ibarretxe-Bilbao *et al.* 2010, 2011b], but not others [Meppelink *et al.* 2010]. Olfactory dysfunction was related to grey matter atrophy in olfactory regions including the piriform cortex and amygdala [Wattendorf *et al.* 2009]. Nonmotor symptoms were thus associated with structural changes in specific related brain networks.

Morphometric and signal changes in other Parkinsonian syndromes

Volumetric MRI was efficient for differentiating Parkinsonian disorders such as progressive supranuclear palsy (PSP) and the Parkinson variant of multiple system atrophy (MSA-P) from PD. There changes were reviewed extensively [Seppi and Poewe, 2010]. In contrast to PD, where structural changes are subtle or absent, PSP patients present with extensive atrophy in the brainstem, basal ganglia and cortex. Midbrain atrophy in PSP has a characteristic shape described as the 'penguin' or 'hummingbird' sign [Kato *et al.* 2003; Righini *et al.* 2004] and can be quantified using various indexes [Oba *et al.* 2005; Paviour *et al.* 2006; Quattrone *et al.* 2008; Righini *et al.* 2004]. Using VBM, grey and white matter reductions have been constantly reported in PSP in the midbrain and more variably in the basal ganglia, the frontal cortex, the insula and the thalamus [Boxer *et al.* 2006; Brenneis *et al.* 2004; Cordato *et al.* 2005; Josephs *et al.* 2008; Lehericy *et al.* 2010; Messina *et al.* 2011; Padovani *et al.* 2006]. In MSA-P, atrophy and signal changes were observed in the putamen (hypointensity in the dorsolateral part and hyperintense rim around the putamen), the pons (cross sign), the middle cerebellar peduncle (T2 hyperintensity) and the cerebellum [Seppi and Poewe, 2010]. PSP patients had greater midbrain and superior cerebellar atrophy whereas MSA-P patients had greater pontine and middle cerebellar atrophy [Oba *et al.* 2005; Paviour *et al.* 2006; Quattrone *et al.* 2008; Righini *et al.* 2004]. In MSA-P patients atrophy was also evidenced in the cortex using VBM [Brenneis *et al.* 2003; Minnerop *et al.* 2007]. Quantitative volumetric measures of pontine and midbrain areas [Oba *et al.* 2005; Quattrone *et al.* 2008] were able to discriminate accurately PSP and MSA-P from PD patients or healthy controls.

Iron load

Iron load may be estimated using measurements of T2 and T2* relaxation times and more recently, using SWI (Table 1). T2 relaxation times characterize how fast water magnetization returns to equilibrium after perturbation by a radiofrequency pulse during an MRI sequence. R2 relaxation rates correspond to 1/T2. T2 relaxation times are characteristic of tissue composition and depend on its molecular structure. The apparent transverse relaxation time T2* (T2 star) is sensitive to the macroscopic and microscopic inhomogeneities of the magnetic field. Macroscopic inhomogeneities are linked to hardware imperfections or to the presence of tissue interfaces characterized by a significant gradient of susceptibility. Microscopic inhomogeneities are linked to the tissue microstructure. Many experiments have shown that T2/R2 and T2*/R2* relaxation rates are noninvasive estimates of iron content either in primate or postmortem studies in humans, with better results obtained using R2* [Hardy *et al.* 2005; Langkammer *et al.* 2010; Ordidge *et al.* 1994]. Improved relaxation measurement techniques have recently been proposed based on adiabatic pulse sequences (T1ρ and T2ρ) [Menke *et al.* 2010; Michaeli *et al.* 2005, 2007]. Changes in iron concentration also result in changes in the phase of the tissue relative to its surroundings, a property which is used in SWI to quantify iron load [Haacke *et al.* 2005; Lotfipour *et al.* 2012; Schafer *et al.* 2012; Wang *et al.* 2012] (Table 1).

In PD iron load is increased [Dexter *et al.* 1989]. T2 relaxometry has provided largely consistent and reproducible results with decreased T2/T2*/adiabatic T2ρ relaxation times and increased R2/R2* relaxation rates [Baudrexel *et al.* 2010; Dexter *et al.* 1989; Du *et al.* 2011; Graham *et al.* 2000; Martin *et al.* 2008; Michaeli *et al.* 2007;

Ordidge *et al.* 1994; Peran *et al.* 2010; Wang *et al.* 2012; Zhang *et al.* 2010]. However, some studies observed a change in T2 only in a particular subgroup [Ordidge *et al.* 1994] or no change at all. A predominance of R2* changes in the lateral SNc [Martin *et al.* 2008], in line with the location of predominant cell loss reported in histological studies [Damier *et al.* 1999]. Changes in R2* in the SN correlated with the motor score of the UPDRS [Martin *et al.* 2008] or with the levodopa equivalent daily dose scores [Peran *et al.* 2010].

In PSP [Boelmans *et al.* 2012] and MSA-P, changes in T2 relaxation times affected more widespread regions including the striatum and the GP as shown using phase-contrast susceptibility imaging [Wang *et al.* 2012] or relaxometry [Arabia *et al.* 2010; Boelmans *et al.* 2012].

Other quantitative biomarkers

In addition to relaxation times and rates, other quantitative markers include magnetization transfer ratio (MTR) and diffusion metrics such as fractional anisotropy (FA) and mean diffusivity (MD).

Magnetization transfer

MT imaging is a technique which relies on the transfer of energy between highly bound protons, e.g. linked to macromolecules, and mobile protons, i.e. in free water [Wolff and Balaban, 1989] (Table 1). Highly bound protons linked to macromolecules are present within structures such as myelin. The amount of MT is thus considered to correlate with the degree of myelination [Rademacher *et al.* 1999] and axonal density [van Waesberghe *et al.* 1999]. MT is therefore used in diseases such as multiple sclerosis [Dousset *et al.* 1992]. MT provides a quantitative parameter, the MTR [Dousset *et al.* 1992]. The MTR was reduced in the SN as well as in other basal ganglia (GP, the putamen, caudate nucleus) in PD patients [Eckert *et al.* 2004; Tambasco *et al.* 2011].

Water diffusion

Diffusion MRI is technique that is sensitive to water diffusion in biological tissues [Le Bihan, 2003]. Diffusion MRI provides several indexes that characterize the overall displacement of molecules (apparent diffusion coefficient [ADC] and MD), the orientation of diffusion (FA) and the characteristics of diffusion along the main direction of diffusion (axial or longitudinal diffusivity) and perpendicular to it (radial or transverse diffusivity) [Le Bihan, 2003]. At the cellular level, anisotropy may result from the presence of obstacles to diffusion due to oriented structures such as the membrane, myelin, longitudinal filaments and cytoskeleton [Le Bihan, 2003]. Changes in axial diffusivity may reflect axonal damage whereas changes in radial diffusivity may reflect myelin damage. Although efforts are pursued to develop methods that better characterize brain changes [Alexander, 2008; Assaf *et al.* 2008; Jensen *et al.* 2005; Zhang *et al.* 2012], to date diffusion parameters suffer from a lack of specificity and poor knowledge of the underlying neuronal substrates.

In the SN of PD patients, changes in the orientation of diffusion, i.e. anisotropy, appeared more consistent than changes in diffusivity (Table 1). Most studies reported reduced anisotropy in early PD patients [Chan *et al.* 2007; Du *et al.* 2011; Peran *et al.* 2010; Vaillancourt *et al.* 2009; Yoshikawa *et al.* 2004; Zhan *et al.* 2012], however others did not [Menke *et al.* 2009, 2010]. Changes in diffusion kurtosis, a method that quantifies non-Gaussian water diffusion [Jensen *et al.* 2005] were also reported in PD patients [Wang *et al.* 2011]. In contrast, diffusivity was mostly unchanged in PD patients [Seppi and Poewe, 2010; Seppi and Schocke, 2005]. Reduction in FA in the SN inversely correlated with clinical severity in some studies [Chan *et al.* 2007; Zhan *et al.* 2012] but not in other studies [Du *et al.* 2011].

In the striatum, diffusion measures were most often normal [Cochrane and Ebmeier, 2013; Nicoletti *et al.* 2006; Paviour *et al.* 2007] although few studies reported increased diffusivity in the striatum and thalamus in PD [Peran *et al.* 2010; Zhan *et al.* 2012].

Diffusion imaging is also useful to discriminate PD from other Parkinsonian syndromes [Cochrane and Ebmeier, 2013]. In PSP, diffusivity was increased in the basal ganglia [Rizzo *et al.* 2008; Seppi *et al.* 2003], the midbrain [Blain *et al.* 2006; Seppi and Poewe, 2010; Seppi and Schocke, 2005], the superior cerebellar peduncle [Nicoletti *et al.* 2008], the precentral white matter [Ohshita *et al.* 2000] and the total white matter [Padovani *et al.* 2006]. In MSA-P, diffusivity was increased and anisotropy was decreased in the putamen,

pons and middle cerebellar peduncle [Blain *et al.* 2006; Nicoletti *et al.* 2006; Paviour *et al.* 2007; Schocke *et al.* 2004] and MTR was reduced in the putamen [Eckert *et al.* 2004].

Differential diagnosis of Parkinsonian syndromes using quantitative biomarkers

Several studies have suggested that the combination of R2* and FA markers may better differentiate people with PD from healthy aged subjects with greater than 95% global accuracy [Du *et al.* 2011; Peran *et al.* 2010].

In PSP, increased diffusivity and reduction in T2 relaxation times were widespread involving the basal ganglia [Boelmans *et al.* 2012; Rizzo *et al.* 2008; Seppi *et al.* 2003], the midbrain [Blain *et al.* 2006; Seppi and Poewe, 2010; Seppi and Schocke, 2005], the superior cerebellar peduncle [Nicoletti *et al.* 2008] and the white matter [Ohshita *et al.* 2000; Padovani *et al.* 2006].

In MSA-P, increased diffusivity and reduced anisotropy was found in the putamen, pons and middle cerebellar peduncle [Blain *et al.* 2006; Nicoletti *et al.* 2006; Paviour *et al.* 2007; Schocke *et al.* 2004] and greater iron deposition in the putamen, using phase-contrast susceptibility imaging [Wang *et al.* 2012] or relaxometry [Arabia *et al.* 2010; Boelmans *et al.* 2012].

Tractography and anatomical connectivity

Tractography is a technique based on the anisotropy of water diffusion that allows reconstructing fibre tracts in the brain. Tracks are reconstructed by assuming that the main direction of diffusion in a voxel indicates the local orientation of white matter fibres [Dell'acqua and Catani, 2012; Mori *et al.* 1999]. Using tractography, diffusion measures (MD, FA) and connectivity measures (e.g. the number of tracks or connection probability between brain regions) can be calculated within the specific fibre tracks. Tractography has also been successfully used to parcel out the SN [Menke *et al.* 2009] and the basal ganglia into specific territories [Draganski *et al.* 2008; Lehericy *et al.* 2004].

In PD, reduced connectivity was observed between the SN and ipsilateral putamen and thalamus [Menke *et al.* 2009; Sharman *et al.* 2012] as well as in the sensorimotor circuit of the basal ganglia [Sharman *et al.* 2012] (Table 1). Automated diffusion-based parcellation of SN subregions showed that the SNr and SNc in PD patients showed a general atrophy [Menke *et al.* 2010]. Tractography is therefore used to investigate changes in anatomical connectivity in PD patients [Menke *et al.* 2009, 2010; Sharman *et al.* 2012].

Perfusion

Perfusion can be assessed noninvasively with MRI without contrast agent administration using arterial spin labelled (ASL) techniques [Detre *et al.* 1992]. ASL techniques have been recently introduced as a noninvasive alternative to PET or SPECT imaging for perfusion measurements in PD [Fernandez-Seara *et al.* 2012; Kamagata *et al.* 2011; Ma *et al.* 2010; Melzer *et al.* 2011]. In ASL, the tracer is endogenous arterial blood water that is labelled electromagnetically using radiofrequency (RF) irradiation [Detre *et al.* 2012]. ASL perfusion imaging provides quantitative measurements of cerebral blood flow [Detre *et al.* 2012].

Compared with healthy controls, perfusion in PD was decreased in the cortex [Fernandez-Seara *et al.* 2012; Kamagata *et al.* 2011; Melzer *et al.* 2011] and either preserved [Melzer *et al.* 2011] or decreased [Fernandez-Seara *et al.* 2012] in the basal ganglia and preserved in the sensorimotor areas [Melzer *et al.* 2011] (Table 1). Perfusion patterns were correlated with metabolic changes using fluorodeoxyglucose PET [Ma *et al.* 2010].

Metabolic biomarkers

Proton magnetic resonance spectroscopy (^{1}H MRS) provides information about the levels of metabolites in the brain (Table 1). Metabolites that are evaluated include *N*-acetylaspartate (NAA; considered as a marker of neuronal number and health), choline-containing compounds (Cho; markers of demyelination and cell proliferation), *myo*-inositol (mIns; considered as a marker for osmotic stress or astrogliosis), lactate (frequently associated brain pathologies), glutathione (GSH) as well as neurotransmitters such as glutamate/glutamine or GABA (using specific editing techniques). Metabolite levels may be reported as their ratios over sum of creatine and phosphocreatine (Cr; which used a concentration reference) or as absolute concentrations. MRS is highly sensitive to magnetic field homogeneity and lipid artefact signals when the regions examined are too close to the skull. MRS of the SN is therefore

very challenging in humans due to the location, small size and high iron content of the structure. Regions studied present partial voluming with the rest of the midbrain.

Using ^{1}H-MRS, two groups reported changes in metabolites at 3T [Groger *et al.* 2011; Hattingen *et al.* 2009]. This was not confirmed at higher field as MRS at 4T [Oz *et al.* 2006] or 7T [Emir *et al.* 2012] did not show significant changes in the SN of PD patients. The authors only report a trend for Glu, NAA and GSH to decrease, and for Cho to increase [Oz *et al.* 2006].

Phosphorus magnetic resonance spectroscopy (^{31}P MRS) allows direct monitoring of the energy metabolism of the brain [Ross and Bluml, 2001] (Table 1). PD patients showed abnormal phosphate metabolisms [Barbiroli *et al.* 1999; Hattingen *et al.* 2009; Hu *et al.* 2000] that suggested mitochondrial dysfunction of mesostriatal neurons [Barbiroli *et al.* 1999; Hattingen *et al.* 2009; Hu *et al.* 2000; Rango *et al.* 2006].

Functional connectivity

Initially designed to detect task-related signal changes in the brain, blood oxygen level-dependent (BOLD) fMRI is also increasingly used to study functional connectivity between distant brain regions. Spatially remote regions forming distributed cortical and subcortical networks can present temporal correlations of the fluctuations of their fMRI signal at rest [Biswal *et al.* 1995; Friston *et al.* 1993]. These networks are extracted from rsfMRI data using various mathematical approaches [Bullmore and Sporns, 2009; Ramnani *et al.* 2004] (Table 1).

Functional interactions in resting brain networks are abnormal in PD [Helmich *et al.* 2009; Hacker *et al.* 2012; Sharman *et al.* 2012; Skidmore *et al.* 2011b; Wu *et al.* 2011]. rsfMRI studies have shown that PD is associated with changes in cerebral connectivity between the basal ganglia and the cortex or cerebellum [Helmich *et al.* 2009] and between the STN and cortical motor and premotor areas [Baudrexel *et al.* 2011]. Changes predominate in the sensorimotor circuit with decreased functional coupling whereas functional connectivity was increased in the associative territory [Sharman *et al.* 2012; Hacker *et al.* 2012; Helmich *et al.* 2009]. Abnormal functional connectivity was also evidenced in the default-mode network in cognitively unimpaired PD patients that correlated with cognitive performances in memory and visuospatial tests [Tessitore *et al.* 2012b]. In drug-naïve PD patients, the supplementary motor area showed reduced signal fluctuations in PD whereas levodopa enhanced functional connectivity in this region [Esposito *et al.* 2013]. Changes were observed in a specific frequency band [Esposito *et al.* 2013]. Changes in resting state BOLD fluctuations were successful in predicting the presence of PD [Long *et al.* 2012; Skidmore *et al.* 2011b].

Changes in functional connectivity were differently associated with symptoms in PD. Tremor has been related to increased functional connectivity between the STN and the primary sensorimotor area [Baudrexel *et al.* 2011] and to abnormal functional interactions between the basal ganglia and the cerebello-thalamic circuit [Helmich *et al.* 2011]. Apathy was related to abnormal functional connectivity in the orbitofrontal, supplementary motor and middle frontal areas [Skidmore *et al.* 2011a]. In contrast, depression was associated with functional connectivity changes in the subgenual cingulate cortex [Skidmore *et al.* 2011a]. Increased amplitude of low-frequency BOLD signal oscillations in the premotor cortex predicted motor performances [Kwak *et al.* 2012].

In PSP, rsfMRI showed connectivity disruptions between the dorsal midbrain tegmentum and the cerebellum, diencephalum, basal ganglia and cortex that were associated with more severe functional impairment [Gardner *et al.* 2013]. Another study found disconnection between the thalamus and the striatum, supplementary motor area and cerebellum [Whitwell *et al.* 2011].

Overall, findings with resting state fMRI suggest that dopamine depletion in PD leads to a remapping of cerebral connectivity that affects predominantly the sensorimotor circuit and sensorimotor integration, that is influenced by levodopa and differently associated with motor and nonmotor symptoms. rsfMRI methods also showed reduced brainstem and thalamic connectivity in PSP that correlated with clinical deficits.

Conclusion

Over the last decade and a half, research in PD imaging has focused on developing quantitative techniques in the aim of providing measurements that can be used a markers of the disease process.

In the SN, several techniques including diffusion imaging, T2* relaxometry and MT have shown great promises for detecting pathological changes. Investigators have developed computerized neuroanatomical techniques to study cortical changes that have been related to specific motor and non-motor symptoms in the disease. MRI gives also access to the anatomical and functional connectivity changes in the brain of PD patients. MRI techniques could be used to monitor disease progression and to detect brain changes in preclinical patients or in patients at risk of developing PD, such as gait REM sleep behaviour disorder patients. However, to date these techniques suffer from the lack of standardization, particularly methods for extracting quantitative information from images, and of validation in large cohorts of subjects in longitudinal studies. It is expected that future efforts in imaging research will provide significant improvement in this respect.

Funding

This work was supported by 'Investissements d'avenir' (grant number ANR-10-IAIHU-06).

Conflict of interest statement

The authors have no conflicts of interest to declare.

References

Alexander, D. (2008) A general framework for experiment design in diffusion MRI and its application in measuring direct tissue-microstructure features. *Magn Reson Med* 60: 439–448.

Apostolova, L. and Thompson, P. (2007) Brain mapping as a tool to study neurodegeneration. *Neurotherapeutics* 4: 387–400.

Arabia, G., Morelli, M., Paglionico, S., Novellino, F., Salsone, M., Giofre, L. *et al.* (2010) An magnetic resonance imaging T2*-weighted sequence at short echo time to detect putaminal hypointensity in Parkinsonisms. *Mov Disord* 25: 2728–2734.

Ashburner, J. and Friston, K. (2000) Voxel-based morphometry - the methods. *Neuroimage* 11: 805–821.

Assaf, Y., Blumenfeld-Katzir, T., Yovel, Y. and Basser, P. (2008) AxCaliber: a method for measuring axon diameter distribution from diffusion MRI. *Magn Reson Med* 59: 1347–1354.

Barbiroli, B., Martinelli, P., Patuelli, A., Lodi, R., Iotti, S., Cortelli, P. *et al.* (1999) Phosphorus magnetic resonance spectroscopy in multiple system atrophy and Parkinson's disease. *Mov Disord* 14: 430–435.

Baudrexel, S., Nurnberger, L., Rub, U., Seifried, C., Klein, J., Deller, T. *et al.* (2010) Quantitative mapping of T1 and T2* discloses nigral and brainstem pathology in early Parkinson's disease. *Neuroimage* 51: 512–520.

Baudrexel, S., Witte, T., Seifried, C., von Wegner, F., Beissner, F., Klein, J. *et al.* (2011) Resting state fMRI reveals increased subthalamic nucleus-motor cortex connectivity in Parkinson's disease. *Neuroimage* 55: 1728–1738.

Beyer, M., Janvin, C., Larsen, J. and Aarsland, D. (2007) A magnetic resonance imaging study of patients with Parkinson's disease with mild cognitive impairment and dementia using voxel-based morphometry. *J Neurol Neurosurg Psychiatry* 78: 254–259.

Biswal, B., Yetkin, F., Haughton, V. and Hyde, J. (1995) Functional connectivity in the motor cortex of resting human brain using echo-planar MRI. *Magn Reson Med* 34: 537–541.

Biundo, R., Formento-Dojot, P., Facchini, S., Vallelunga, A., Ghezzo, L., Foscolo, L. *et al.* (2011) Brain volume changes in Parkinson's disease and their relationship with cognitive and behavioural abnormalities. *J Neurol Sci* 310: 64–69.

Blain, C., Barker, G., Jarosz, J., Coyle, N., Landau, S., Brown, R. *et al.* (2006) Measuring brain stem and cerebellar damage in parkinsonian syndromes using diffusion tensor MRI. *Neurology* 67: 2199–2205.

Boelmans, K., Holst, B., Hackius, M., Finsterbusch, J., Gerloff, C., Fiehler, J. *et al.* (2012) Brain iron deposition fingerprints in Parkinson's disease and progressive supranuclear palsy. *Mov Disord* 27: 421–427.

Bonneville, F., Welter, M., Elie, C., du Montcel, S., Hasboun, D., Menuel, C. *et al.* (2005) Parkinson disease, brain volumes, and subthalamic nucleus stimulation. *Neurology* 64: 1598–1604.

Boxer, A., Geschwind, M., Belfor, N., Gorno-Tempini, M., Schauer, G., Miller, B. *et al.* (2006) Patterns of brain atrophy that differentiate corticobasal degeneration syndrome from progressive supranuclear palsy. *Arch Neurol* 63: 81–86.

Brenneis, C., Seppi, K., Schocke, M., Benke, T., Wenning, G. and Poewe, W. (2004) Voxel based morphometry reveals a distinct pattern of frontal atrophy in progressive supranuclear palsy. *J Neurol Neurosurg Psychiatry* 75: 246–249.

Brenneis, C., Seppi, K., Schocke, M., Muller, J., Luginger, E., Bosch, S. *et al.* (2003) Voxel-based morphometry detects cortical atrophy in the Parkinson variant of multiple system atrophy. *Mov Disord* 18: 1132–1138.

Brooks, D. and Pavese, N. (2010) Imaging non-motor aspects of Parkinson's disease. *Prog Brain Res* 184: 205–218.

Bullmore, E. and Sporns, O. (2009) Complex brain networks: graph theoretical analysis of structural and functional systems. *Nat Rev Neurosci* 10: 186–198.

Burton, E., McKeith, I., Burn, D., Williams, E. and O'Brien, J. (2004) Cerebral atrophy in Parkinson's disease with and without dementia: a comparison with Alzheimer's disease, dementia with Lewy bodies and controls. *Brain* 127: 791–800.

Cardoso, E., Maia, F., Fregni, F., Myczkowski, M., Melo, L., Sato, J. *et al.* (2009) Depression in Parkinson's disease: convergence from voxel-based morphometry and functional magnetic resonance imaging in the limbic thalamus. *Neuroimage* 47: 467–472.

Cerasa, A., Messina, D., Pugliese, P., Morelli, M., Lanza, P., Salsone, M. *et al.* (2011) Increased prefrontal volume in PD with levodopa-induced dyskinesias: a voxel-based morphometry study. *Mov Disord* 26: 807–812.

Chan, L., Rumpel, H., Yap, K., Lee, E., Loo, H., Ho, G. *et al.* (2007) Case control study of diffusion tensor imaging in Parkinson's disease. *J Neurol Neurosurg Psychiatry* 78: 1383–1386.

Cho, Z., Oh, S., Kim, J., Park, S., Kwon, D., Jeong, H. *et al.* (2011) Direct visualization of Parkinson's disease by in vivo human brain imaging using 7.0T magnetic resonance imaging. *Mov Disord* 26: 713–718.

Cochrane, C. and Ebmeier, K. (2013) Diffusion tensor imaging in parkinsonian syndromes: a systematic review and meta-analysis. *Neurology* 80: 857–864.

Cordato, N., Duggins, A., Halliday, G., Morris, J. and Pantelis, C. (2005) Clinical deficits correlate with regional cerebral atrophy in progressive supranuclear palsy. *Brain* 128: 1259–1266.

Dale, A., Fischl, B. and Sereno, M. (1999) Cortical surface-based analysis. I. Segmentation and surface reconstruction. *Neuroimage* 9: 179–194.

Damier, P., Hirsch, E., Agid, Y. and Graybiel, A. (1999) The substantia nigra of the human brain. II. Patterns of loss of dopamine-containing neurons in Parkinson's disease. *Brain* 122: 1437–1448.

Dell'acqua, F. and Catani, M. (2012) Structural human brain networks: hot topics in diffusion tractography. *Curr Opin Neurol* 25: 375–383.

Destrieux, C., Fischl, B., Dale, A. and Halgren, E. (2010) Automatic parcellation of human cortical gyri and sulci using standard anatomical nomenclature. *Neuroimage* 53: 1–15.

Detre, J., Leigh, J., Williams, D. and Koretsky, A. (1992) Perfusion imaging. *Magn Reson Med* 23: 37–45.

Detre, J., Rao, H., Wang, D., Chen, Y. and Wang, Z. (2012) Applications of arterial spin labeled MRI in the brain. *J Magn Reson Imaging* 35: 1026–1037.

Dexter, D., Wells, F., Lees, A., Agid, F., Agid, Y., Jenner, P. *et al.* (1989) Increased nigral iron content and alterations in other metal ions occurring in brain in Parkinson's disease. *J Neurochem* 52: 1830–1836.

Dousset, V., Grossman, R., Ramer, K., Schnall, M., Young, L., Gonzalez-Scarano, F. *et al.* (1992) Experimental allergic encephalomyelitis and multiple sclerosis: lesion characterization with magnetization transfer imaging. *Radiology* 182: 483–491.

Draganski, B., Kherif, F., Kloppel, S., Cook, P., Alexander, D., Parker, G. *et al.* (2008) Evidence for segregated and integrative connectivity patterns in the human basal ganglia. *J Neurosci* 28: 7143–7152.

Du, G., Lewis, M., Styner, M., Shaffer, M., Sen, S., Yang, Q. *et al.* (2011) Combined R2* and diffusion tensor imaging changes in the substantia nigra in Parkinson's disease. *Mov Disord* 26: 1627–1632.

Eckert, T., Sailer, M., Kaufmann, J., Schrader, C., Peschel, T., Bodammer, N. *et al.* (2004) Differentiation of idiopathic Parkinson's disease, multiple system atrophy, progressive supranuclear palsy, and healthy controls using magnetization transfer imaging. *Neuroimage* 21: 229–235.

Emir, U., Tuite, P. and Oz, G. (2012) Elevated pontine and putamenal GABA levels in mild-moderate Parkinson disease detected by 7 Tesla proton MRS. *PLoS One* 7(1): e30918.

Esposito, F., Tessitore, A., Giordano, A., De Micco, R., Paccone, A., Conforti, R. *et al.* (2013) Rhythm-specific modulation of the sensorimotor network in drug-naive patients with Parkinson's disease by levodopa. *Brain* 136: 710–725.

Feldmann, A., Illes, Z., Kosztolanyi, P., Illes, E., Mike, A., Kover, F. *et al.* (2008) Morphometric changes of gray matter in Parkinson's disease with depression: a voxel-based morphometry study. *Mov Disord* 23: 42–46.

Fernandez-Seara, M., Mengual, E., Vidorreta, M., Aznarez-Sanado, M., Loayza, F., Villagra, F. *et al.* (2012) Cortical hypoperfusion in Parkinson's disease assessed using arterial spin labeled perfusion MRI. *Neuroimage* 59: 2743–2750.

Fischl, B., Sereno, M. and Dale, A. (1999) Cortical surface-based analysis. II: Inflation, flattening, and a surface-based coordinate system. *Neuroimage* 9: 195–207.

Friston, K., Frith, C., Liddle, P. and Frackowiak, R. (1993) Functional connectivity: the principal-component analysis of large (PET) data sets. *J Cereb Blood Flow Metab* 13: 5–14.

Garcia-Lorenzo, D., Longo-Dos Santos, C., Ewenczyk, C., Leu-Semenescu, S., Gallea, C., Quattrocchi, G. *et al.* (2013) The coeruleus/subcoeruleus complex in rapid eye movement sleep behaviour disorders in Parkinson's disease. *Brain* 136: 2120–2129.

Gardner, R., Boxer, A., Trujillo, A., Mirsky, J., Guo, C., Gennatas, E. *et al.* (2013) Intrinsic connectivity network disruption in progressive supranuclear palsy. *Ann Neurol* 73: 603–616.

Good, C., Ashburner, J. and Frackowiak, R. (2001) Computational neuroanatomy: new perspectives for neuroradiology. *Rev Neurol (Paris)* 157: 797–806.

Graham, J., Paley, M., Grunewald, R., Hoggard, N. and Griffiths, P. (2000) Brain iron deposition in Parkinson's disease imaged using the PRIME magnetic resonance sequence. *Brain* 123: 2423–2431.

Groger, A., Chadzynski, G., Godau, J., Berg, D. and Klose, U. (2011) Three-dimensional magnetic resonance spectroscopic imaging in the substantia nigra of healthy controls and patients with Parkinson's disease. *Eur Radiol* 21: 1962–1969.

Haacke, E., Cheng, N., House, M., Liu, Q., Neelavalli, J., Ogg, R. *et al.* (2005) Imaging iron stores in the brain using magnetic resonance imaging. *Magn Reson Imaging* 23: 1–25.

Hacker, C., Perlmutter, J., Criswell, S., Ances, B. and Snyder, A. (2012) Resting state functional connectivity of the striatum in Parkinson's disease. *Brain* 135: 3699–3711.

Hardy, P., Gash, D., Yokel, R., Andersen, A., Ai, Y. and Zhang, Z. (2005) Correlation of R2 with total iron concentration in the brains of rhesus monkeys. *J Magn Reson Imaging* 21: 118–127.

Hattingen, E., Magerkurth, J., Pilatus, U., Mozer, A., Seifried, C., Steinmetz, H. *et al.* (2009) Phosphorus and proton magnetic resonance spectroscopy demonstrates mitochondrial dysfunction in early and advanced Parkinson's disease. *Brain* 132: 3285–3297.

Helmich, R., Derikx, L., Bakker, M., Scheeringa, R., Bloem, B. and Toni, I. (2009) Spatial remapping of cortico-striatal connectivity in Parkinson's disease. *Cereb Cortex* 20: 1175–1186.

Helmich, R., Janssen, M., Oyen, W., Bloem, B. and Toni, I. (2011) Pallidal dysfunction drives a cerebellothalamic circuit into Parkinson tremor. *Ann Neurol* 69: 269–281.

Helms, G., Draganski, B., Frackowiak, R., Ashburner, J. and Weiskopf, N. (2009) Improved segmentation of deep brain grey matter structures using magnetization transfer (MT) parameter maps. *Neuroimage* 47: 194–198.

Hu, M., Taylor-Robinson, S., Chaudhuri, K., Bell, J., Labbe, C., Cunningham, V. *et al.* (2000) Cortical dysfunction in non-demented Parkinson's disease patients: a combined (31)P-MRS and (18)FDG-PET study. *Brain* 123: 340–352.

Hutchinson, M., Raff, U. and Lebedev, S. (2003) MRI correlates of pathology in Parkinsonism: segmented inversion recovery ratio imaging (SIRRIM). *Neuroimage* 20: 1899–1902.

Ibarretxe-Bilbao, N., Junque, C., Marti, M. and Tolosa, E. (2011a) Brain structural MRI correlates of cognitive dysfunctions in Parkinson's disease. *J Neurol Sci* 310: 70–74.

Ibarretxe-Bilbao, N., Junque, C., Marti, M. and Tolosa, E. (2011b) Cerebral basis of visual hallucinations in Parkinson's disease: structural and functional MRI studies. *J Neurol Sci* 310: 79–81.

Ibarretxe-Bilbao, N., Junque, C., Segura, B., Baggio, H., Marti, M., Valldeoriola, F. *et al.* (2012) Progression of cortical thinning in early Parkinson's disease. *Mov Disord* 27: 1746–1753.

Ibarretxe-Bilbao, N., Ramirez-Ruiz, B., Junque, C., Marti, M., Valldeoriola, F., Bargallo, N. *et al.* (2010) Differential progression of brain atrophy in Parkinson's disease with and without visual hallucinations. *J Neurol Neurosurg Psychiatry* 81: 650–657.

Ibarretxe-Bilbao, N., Tolosa, E., Junque, C. and Marti, M. (2009) MRI and cognitive impairment in Parkinson's disease. *Mov Disord* 24(Suppl. 2): S748–S753.

Jensen, J., Helpern, J., Ramani, A., Lu, H. and Kaczynski, K. (2005) Diffusional kurtosis imaging: the quantification of non-Gaussian water diffusion by means of magnetic resonance imaging. *Magn Reson Med* 53: 1432–1440.

Josephs, K., Whitwell, J., Dickson, D., Boeve, B., Knopman, D., Petersen, R. *et al.* (2008) Voxel-based morphometry in autopsy proven PSP and CBD. *Neurobiol Aging* 29: 280–289.

Jubault, T., Gagnon, J., Karama, S., Ptito, A., Lafontaine, A., Evans, A. *et al.* (2011) Patterns of cortical thickness and surface area in early Parkinson's disease. *Neuroimage* 55: 462–467.

Kamagata, K., Motoi, Y., Hori, M., Suzuki, M., Nakanishi, A., Shimoji, K. *et al.* (2011) Posterior hypoperfusion in Parkinson's disease with and without dementia measured with arterial spin labeling MRI. *J Magn Reson Imaging* 33: 803–807.

Karagulle Kendi, A., Lehericy, S., Luciana, M., Ugurbil, K. and Tuite, P. (2008) Altered diffusion

in the frontal lobe in Parkinson disease. *AJNR Am J Neuroradiol* 29: 501–505.

Kato, N., Arai, K. and Hattori, T. (2003) Study of the rostral midbrain atrophy in progressive supranuclear palsy. *J Neurol Sci* 210: 57–60.

Kostic, V., Agosta, F., Petrovic, I., Galantucci, S., Spica, V., Jecmenica-Lukic, M. *et al.* (2010) Regional patterns of brain tissue loss associated with depression in Parkinson disease. *Neurology* 75: 857–863.

Kwak, Y., Peltier, S., Bohnen, N., Muller, M., Dayalu, P. and Seidler, R. (2012) L-DOPA changes spontaneous low-frequency BOLD signal oscillations in Parkinson's disease: a resting state fMRI study. *Front Syst Neurosci* 6: 52.

Kwon, D., Kim, J., Oh, S., Jeong, H., Park, S., Oh, E. *et al.* (2012) Seven-Tesla magnetic resonance images of the substantia nigra in Parkinson disease. *Ann Neurol* 71: 267–277.

Langkammer, C., Krebs, N., Goessler, W., Scheurer, E., Ebner, F., Yen, K. *et al.* (2010) Quantitative MR imaging of brain iron: a postmortem validation study. *Radiology* 257: 455–462.

Le Bihan, D. (2003) Looking into the functional architecture of the brain with diffusion MRI. *Nat Rev Neurosci* 4: 469–480.

Lehericy, S., Ducros, M., Van, de, Moortele, P., Francois, C., Thivard, L., Poupon, C. *et al.* (2004) Diffusion tensor fiber tracking shows distinct corticostriatal circuits in humans. *Ann Neurol* 55: 522–529.

Lehericy, S., Hartmann, A., Lannuzel, A., Galanaud, D., Delmaire, C., Bienaimee, M. *et al.* (2010) Magnetic resonance imaging lesion pattern in Guadeloupean Parkinsonism is distinct from progressive supranuclear palsy. *Brain* 133: 2410–2425.

Litvan, I., Aarsland, D., Adler, C., Goldman, J., Kulisevsky, J., Mollenhauer, B. *et al.* (2011) MDS Task Force on mild cognitive impairment in Parkinson's disease: critical review of PD-MCI. *Mov Disord* 26: 1814–1824.

Long, D., Wang, J., Xuan, M., Gu, Q., Xu, X., Kong, D. *et al.* (2012) Automatic classification of early Parkinson's disease with multi-modal MR imaging. *PLoS One* 7(11): e47714.

Longoni, G., Agosta, F., Kostic, V., Stojkovic, T., Pagani, E., Stosic-Opincal, T. *et al.* (2011) MRI measurements of brainstem structures in patients with Richardson's syndrome, progressive supranuclear palsy-parkinsonism, and Parkinson's disease. *Mov Disord* 26: 247–255.

Lotfipour, A., Wharton, S., Schwarz, S., Gontu, V., Schafer, A., Peters, A. *et al.* (2012) High resolution magnetic susceptibility mapping of the substantia nigra in Parkinson's disease. *J Magn Reson Imaging* 35: 48–55.

Lyoo, C., Ryu, Y. and Lee, M. (2010) Topographical distribution of cerebral cortical thinning in patients with mild Parkinson's disease without dementia. *Mov Disord* 25: 496–499.

Ma, Y., Huang, C., Dyke, J., Pan, H., Alsop, D., Feigin, A. *et al.* (2010) Parkinson's disease spatial covariance pattern: noninvasive quantification with perfusion MRI. *J Cereb Blood Flow Metab* 30: 505–509.

Makris, N., Schlerf, J., Hodge, S., Haselgrove, C., Albaugh, M., Seidman, L. *et al.* (2005) MRI-based surface-assisted parcellation of human cerebellar cortex: an anatomically specified method with estimate of reliability. *Neuroimage* 25: 1146–1160.

Martin, W., Wieler, M. and Gee, M. (2008) Midbrain iron content in early Parkinson disease: a potential biomarker of disease status. *Neurology* 70: 1411–1417.

Melzer, T., Watts, R., MacAskill, M., Pearson, J., Rueger, S., Pitcher, T. *et al.* (2011) Arterial spin labelling reveals an abnormal cerebral perfusion pattern in Parkinson's disease. *Brain* 134: 845–855.

Menke, R., Jbabdi, S., Miller, K., Matthews, P. and Zarei, M. (2010) Connectivity-based segmentation of the substantia nigra in human and its implications in Parkinson's disease. *Neuroimage* 52: 1175–1180.

Menke, R., Scholz, J., Miller, K., Deoni, S., Jbabdi, S., Matthews, P. *et al.* (2009) MRI characteristics of the substantia nigra in Parkinson's disease: a combined quantitative T1 and DTI study. *Neuroimage* 47: 435–441.

Meppelink, A., de Jong, B., Teune, L. and van Laar, T. (2010) Regional cortical grey matter loss in Parkinson's disease without dementia is independent from visual hallucinations. *Mov Disord* 26: 142–147.

Messina, D., Cerasa, A., Condino, F., Arabia, G., Novellino, F., Nicoletti, G. *et al.* (2011) Patterns of brain atrophy in Parkinson's disease, progressive supranuclear palsy and multiple system atrophy. *Parkinsonism Relat Disord* 17: 172–176.

Michaeli, S., Grohn, H., Grohn, O., Sorce, D., Kauppinen, R., Springer, C. Jr *et al.* (2005) Exchange-influenced T2rho contrast in human brain images measured with adiabatic radio frequency pulses. *Magn Reson Med* 53: 823–829.

Michaeli, S., Oz, G., Sorce, D., Garwood, M., Ugurbil, K., Majestic, S. *et al.* (2007) Assessment of brain iron and neuronal integrity in patients with Parkinson's disease using novel MRI contrasts. *Mov Disord* 22: 334–340.

Minati, L., Grisoli, M., Carella, F., De Simone, T., Bruzzone, M. and Savoiardo, M. (2007) Imaging

degeneration of the substantia nigra in Parkinson disease with inversion-recovery MR imaging. *AJNR Am J Neuroradiol* 28: 309–313.

Minnerop, M., Specht, K., Ruhlmann, J., Schimke, N., Abele, M., Weyer, A. *et al.* (2007) Voxel-based morphometry and voxel-based relaxometry in multiple system atrophy - a comparison between clinical subtypes and correlations with clinical parameters. *Neuroimage* 36: 1086–1095.

Mori, S., Crain, B., Chacko, V. and van Zijl, P. (1999) Three-dimensional tracking of axonal projections in the brain by magnetic resonance imaging. *Ann Neurol* 45: 265–269.

Nicoletti, G., Lodi, R., Condino, F., Tonon, C., Fera, F., Malucelli, E. *et al.* (2006) Apparent diffusion coefficient measurements of the middle cerebellar peduncle differentiate the Parkinson variant of MSA from Parkinson's disease and progressive supranuclear palsy. *Brain* 129: 2679–2687.

Nicoletti, G., Tonon, C., Lodi, R., Condino, F., Manners, D., Malucelli, E. *et al.* (2008) Apparent diffusion coefficient of the superior cerebellar peduncle differentiates progressive supranuclear palsy from Parkinson's disease. *Mov Disord* 23: 2370–2376.

Oba, H., Yagishita, A., Terada, H., Barkovich, A., Kutomi, K., Yamauchi, T. *et al.* (2005) New and reliable MRI diagnosis for progressive supranuclear palsy. *Neurology* 64: 2050–2055.

Ohshita, T., Oka, M., Imon, Y., Yamaguchi, S., Mimori, Y. and Nakamura, S. (2000) Apparent diffusion coefficient measurements in progressive supranuclear palsy. *Neuroradiology* 42: 643–647.

Oikawa, H., Sasaki, M., Tamakawa, Y., Ehara, S. and Tohyama, K. (2002) The substantia nigra in Parkinson disease: proton density-weighted spin-echo and fast short inversion time inversion-recovery MR findings. *AJNR Am J Neuroradiol* 23: 1747–1756.

Ordidge, R., Gorell, J., Deniau, J., Knight, R. and Helpern, J. (1994) Assessment of relative brain iron concentrations using T2-weighted and T2*-weighted MRI at 3 Tesla. *Magn Reson Med* 32: 335–341.

Oz, G., Terpstra, M., Tkac, I., Aia, P., Lowary, J., Tuite, P. *et al.* (2006) Proton MRS of the unilateral substantia nigra in the human brain at 4 Tesla: detection of high GABA concentrations. *Magn Reson Med* 55: 296–301.

Padovani, A., Borroni, B., Brambati, S., Agosti, C., Broli, M., Alonso, R. *et al.* (2006) Diffusion tensor imaging and voxel based morphometry study in early progressive supranuclear palsy. *J Neurol Neurosurg Psychiatry* 77: 457–463.

Patenaude, B., Smith, S., Kennedy, D. and Jenkinson, M. (2011) A Bayesian model of shape and appearance for subcortical brain segmentation. *Neuroimage* 56: 907–922.

Paviour, D., Price, S., Jahanshahi, M., Lees, A. and Fox, N. (2006) Longitudinal MRI in progressive supranuclear palsy and multiple system atrophy: rates and regions of atrophy. *Brain* 129: 1040–1049.

Paviour, D., Thornton, J., Lees, A. and Jager, H. (2007) Diffusion-weighted magnetic resonance imaging differentiates Parkinsonian variant of multiple-system atrophy from progressive supranuclear palsy. *Mov Disord* 22: 68–74.

Peran, P., Cherubini, A., Assogna, F., Piras, F., Quattrocchi, C., Peppe, A. *et al.* (2010) Magnetic resonance imaging markers of Parkinson's disease nigrostriatal signature. *Brain* 133: 3423–3433.

Quattrone, A., Nicoletti, G., Messina, D., Fera, F., Condino, F., Pugliese, P. *et al.* (2008) MR imaging index for differentiation of progressive supranuclear palsy from Parkinson disease and the Parkinson variant of multiple system atrophy. *Radiology* 246: 214–221.

Rademacher, J., Engelbrecht, V., Burgel, U., Freund, H. and Zilles, K. (1999) Measuring in vivo myelination of human white matter fiber tracts with magnetization transfer MR. *Neuroimage* 9: 393–406.

Ramnani, N., Behrens, T., Penny, W. and Matthews, P. (2004) New approaches for exploring anatomical and functional connectivity in the human brain. *Biol Psychiatry* 56: 613–619.

Rango, M., Bonifati, C. and Bresolin, N. (2006) Parkinson's disease and brain mitochondrial dysfunction: a functional phosphorus magnetic resonance spectroscopy study. *J Cereb Blood Flow Metab* 26: 283–290.

Redgrave, P., Rodriguez, M., Smith, Y., Rodriguez-Oroz, M., Lehericy, S., Bergman, H. *et al.* (2010) Goal-directed and habitual control in the basal ganglia: implications for Parkinson's disease. *Nat Rev Neurosci* 11: 760–772.

Righini, A., Antonini, A., De Notaris, R., Bianchini, E., Meucci, N., Sacilotto, G. *et al.* (2004) MR imaging of the superior profile of the midbrain: differential diagnosis between progressive supranuclear palsy and Parkinson disease. *AJNR Am J Neuroradiol* 25: 927–932.

Rizzo, G., Martinelli, P., Manners, D., Scaglione, C., Tonon, C., Cortelli, P. *et al.* (2008) Diffusion-weighted brain imaging study of patients with clinical diagnosis of corticobasal degeneration, progressive supranuclear palsy and Parkinson's disease. *Brain* 131: 2690–2700.

Ross, B. and Bluml, S. (2001) Magnetic resonance spectroscopy of the human brain. *Anat Rec* 265(2): 54–84.

Sasaki, M., Shibata, E., Tohyama, K., Takahashi, J., Otsuka, K., Tsuchiya, K. *et al.* (2006) Neuromelanin magnetic resonance imaging of locus ceruleus and substantia nigra in Parkinson's disease. *Neuroreport* 17: 1215–1218.

Schafer, A., Forstmann, B., Neumann, J., Wharton, S., Mietke, A., Bowtell, R. *et al.* (2012) Direct visualization of the subthalamic nucleus and its iron distribution using high-resolution susceptibility mapping. *Hum Brain Mapp* 33: 2831–2842.

Schocke, M., Seppi, K., Esterhammer, R., Kremser, C., Mair, K., Czermak, B. *et al.* (2004) Trace of diffusion tensor differentiates the Parkinson variant of multiple system atrophy and Parkinson's disease. *Neuroimage* 21: 1443–1451.

Seppi, K. and Poewe, W. (2010) Brain magnetic resonance imaging techniques in the diagnosis of parkinsonian syndromes. *Neuroimaging Clin N Am* 20: 29–55.

Seppi, K. and Schocke, M. (2005) An update on conventional and advanced magnetic resonance imaging techniques in the differential diagnosis of neurodegenerative parkinsonism. *Curr Opin Neurol* 18: 370–375.

Seppi, K., Schocke, M., Esterhammer, R., Kremser, C., Brenneis, C., Mueller, J. *et al.* (2003) Diffusion-weighted imaging discriminates progressive supranuclear palsy from PD, but not from the Parkinson variant of multiple system atrophy. *Neurology* 60: 922–927.

Sharman, M., Valabregue, R., Perlbarg, V., Marrakchi-Kacem, L., Vidailhet, M., Benali, H. *et al.* (2012) Parkinson's disease patients show reduced cortical-subcortical sensorimotor connectivity. *Mov Disord*, in press.

Skidmore, F., Yang, M., Baxter, L., von Deneen, K., Collingwood, J., He, G. *et al.* (2011a) Apathy, depression, and motor symptoms have distinct and separable resting activity patterns in idiopathic Parkinson disease. *Neuroimage*, in press.

Skidmore, F., Yang, M., Baxter, L., von Deneen, K., Collingwood, J., He, G. *et al.* (2011b) Reliability analysis of the resting state can sensitively and specifically identify the presence of Parkinson disease. *Neuroimage*, in press.

Svenningsson, P., Westman, E., Ballard, C. and Aarsland, D. (2012) Cognitive impairment in patients with Parkinson's disease: diagnosis, biomarkers, and treatment. *Lancet Neurol* 11: 697–707.

Tambasco, N., Belcastro, V., Sarchielli, P., Floridi, P., Pierguidi, L., Menichetti, C. *et al.* (2011) A magnetization transfer study of mild and advanced Parkinson's disease. *Eur J Neurol* 18: 471–477.

Tessitore, A., Amboni, M., Cirillo, G., Corbo, D., Picillo, M., Russo, A. *et al.* (2012a) Regional gray matter atrophy in patients with Parkinson disease and freezing of gait. *AJNR Am J Neuroradiol*, in press.

Tessitore, A., Esposito, F., Vitale, C., Santangelo, G., Amboni, M., Russo, A. *et al.* (2012b) Default-mode network connectivity in cognitively unimpaired patients with Parkinson disease. *Neurology* 79: 2226–2232.

Tinaz, S., Courtney, M. and Stern, C. (2011) Focal cortical and subcortical atrophy in early Parkinson's disease. *Mov Disord* 26: 436–441.

Vaillancourt, D., Spraker, M., Prodoehl, J., Abraham, I., Corcos, D., Zhou, X. *et al.* (2009) High-resolution diffusion tensor imaging in the substantia nigra of de novo Parkinson disease. *Neurology* 72: 1378–1384.

van Waesberghe, J., Kamphorst, W., De Groot, C., van Walderveen, M., Castelijns, J., Ravid, R. *et al.* (1999) Axonal loss in multiple sclerosis lesions: magnetic resonance imaging insights into substrates of disability. *Ann Neurol* 46: 747–754.

Wang, J., Lin, W., Lu, C., Weng, Y., Ng, S., Wang, C. *et al.* (2011) Parkinson disease: diagnostic utility of diffusion kurtosis imaging. *Radiology* 261: 210–217.

Wang, Y., Butros, S., Shuai, X., Dai, Y., Chen, C., Liu, M. *et al.* (2012) Different iron-deposition patterns of multiple system atrophy with predominant parkinsonism and idiopathetic Parkinson diseases demonstrated by phase-corrected susceptibility-weighted imaging. *AJNR Am J Neuroradiol* 33: 266–273.

Wattendorf, E., Welge-Lussen, A., Fiedler, K., Bilecen, D., Wolfensberger, M., Fuhr, P. *et al.* (2009) Olfactory impairment predicts brain atrophy in Parkinson's disease. *J Neurosci* 29: 15410–15413.

Weintraub, D., Dietz, N., Duda, J., Wolk, D., Doshi, J., Xie, S. *et al.* (2012) Alzheimer's disease pattern of brain atrophy predicts cognitive decline in Parkinson's disease. *Brain* 135: 170–180.

Whitwell, J., Avula, R., Master, A., Vemuri, P., Senjem, M., Jones, D. *et al.* (2011) Disrupted thalamocortical connectivity in PSP: a resting-state fMRI, DTI, and VBM study. *Parkinsonism Relat Disord* 17: 599–605.

Wolff, S. and Balaban, R. (1989) Magnetization transfer contrast (MTC) and tissue water proton relaxation in vivo. *Magn Reson Med* 10: 135–144.

Wu, T., Long, X., Wang, L., Hallett, M., Zang, Y., Li, K. *et al.* (2011) Functional connectivity of cortical motor areas in the resting state in Parkinson's disease. *Hum Brain Mapp* 32: 1443–1457.

Yoshikawa, K., Nakata, Y., Yamada, K. and Nakagawa, M. (2004) Early pathological changes in the parkinsonian brain demonstrated by diffusion tensor MRI. *J Neurol Neurosurg Psychiatry* 75: 481–484.

Zhan, W., Kang, G., Glass, G., Zhang, Y., Shirley, C., Millin, R. *et al.* (2012) Regional alterations of brain microstructure in Parkinson's disease using diffusion tensor imaging. *Mov Disord* 27: 90–97.

Zhang, H., Schneider, T., Wheeler-Kingshott, C. and Alexander, D. (2012) NODDI: practical in vivo neurite orientation dispersion and density imaging of the human brain. *Neuroimage* 61: 1000–1016.

Zhang, J., Zhang, Y., Wang, J., Cai, P., Luo, C., Qian, Z. *et al.* (2010) Characterizing iron deposition in Parkinson's disease using susceptibility-weighted imaging: an in vivo MR study. *Brain Res* 1330: 124–130.